A Novel High Gain Wideband MIMO Antenna for 5G Millimeter Wave Applications

Daniyal Ali Sehrai [1], **Mujeeb Abdullah [2]**, **Ahsan Altaf [3]**, **Saad Hassan Kiani [1]**, **Fazal Muhammad [1,*]**, **Muhammad Tufail [4]**, **Muhammad Irfan [5,*]**, **Adam Glowacz [6]** and **Saifur Rahman [5]**

[1] Department of Electrical Engineering, City University of Science and Information Technology, Peshawar 25000, Pakistan; danyalkhan134@gmail.com (D.A.S.); saad.kiani@cusit.edu.pk (S.H.K.)

[2] Department of Computer Science, Bacha Khan University, Charsadda 24420, Pakistan; mujeeb.abdullah@gmail.com

[3] Department of Electrical Engineering, Istanbul Medipol University, Istanbul 34083, Turkey; aaltaf@st.medipol.edu.tr

[4] Department of Mechatronics Engineering, University of Engineering and Technology, Peshawar 25000, Pakistan; tufail@uetpeshawar.edu.pk

[5] Electrical Engineering Department, College of Engineering, Najran University Saudi Arabia, Najran 61441, Saudi Arabia; srrahman@nu.edu.sa

[6] Department of Automatic, Control and Robotics, AGH University of Science and Technology, 30-059 Krakow, Poland; adglow@agh.edu.pl

* Correspondence: fazal.muhammad@cusit.edu.pk (F.M.); miditta@nu.edu.sa (M.I.)

check for updates

Abstract: A compact tree shape planar quad element Multiple Input Multiple Output (MIMO) antenna bearing a wide bandwidth for 5G communication operating in the millimeter-wave spectrum is proposed. The radiating element of the proposed design contains four different arcs to achieve the wide bandwidth response. Each radiating element is backed by a 1.57 mm thicker Rogers-5880 substrate material, having a loss tangent and relative dielectric constant of 0.0009 and 2.2, respectively. The measured impedance bandwidth of the proposed quad element MIMO antenna system based on 10 dB criterion is from 23 GHz to 40 GHz with a port isolation of greater than 20 dB. The measured radiation patterns are presented at 28 GHz, 33 GHz and 38 GHz with a maximum total gain of 10.58, 8.87 and 11.45 dB, respectively. The high gain of the proposed antenna further helps to overcome the atmospheric attenuations faced by the higher frequencies. In addition, the measured total efficiency of the proposed MIMO antenna is observed above 70% for the millimeter wave frequencies. Furthermore, the MIMO key performance metrics such as Mean Effective Gain (MEG) and Envelope Correlation Coefficient (ECC) are analyzed and found to conform to the required standard of MEG < 3 dB and ECC < 0.5. A prototype of the proposed quad element MIMO antenna system is fabricated and measured. The experimental results validate the simulation design process conducted with Computer Simulation Technology (CST) software.

Keywords: 5G; MIMO; wideband; high isolation; envelope correlation coefficient

1. Introduction

In recent years, Fifth Generation (5G) has acquired a lot of attention in the field of wireless communication. The reason behind the great interest towards the development of the 5G technology is the rapid increase in mobile phone traffic, demanding a higher data rate and bandwidth [1]. So far, the implementation up to 4G technology has been achieved. But these advancements in the technology couldn't fulfil the demand of higher data rate and bandwidth of the modern period [2]. The mobile

data traffic generated from video streaming, social applications and cloud services etc., will probably go beyond the potentials of the current 4G infrastructure before 2020 [3]. Therefore, research has started on the Fifth Generation (5G) technology. After much efforts by researchers, 5G is now being standardized by most countries to accomplish the need for the higher bandwidth and data rates, which is itself a challenging task [4]. To solve this problem, the Multiple Input Multiple Output (MIMO) technologies with a wide bandwidth characteristic are crucial to improve the spectrum efficiency and channel capacity by utilizing the multipath property with no need for increasing the input power [5,6]. Furthermore, the characteristics of high element isolation and broadband should be possessed by the MIMO system to contribute promising performance [7,8]. The higher mutual coupling between the MIMO antenna elements would affect the throughput of the MIMO antenna system [9,10]. Thus, to design a MIMO antenna system with a high element isolation is also a challenge.

The centimeter and millimeter wave spectrum (3–300 GHz) have been mostly targeted by the 5G technology, which can further help to achieve the higher bandwidth with a data rate up to several Gigabit-per-second (Gbps) [11,12]. Another reason for choosing this spectrum range is that the lower spectrum's portion is already under the use of several wireless networks and applications like wireless fidelity (Wi-Fi), Worldwide Interoperability for Microwave Access (WiMAX), Bluetooth, Industrial, Scientific and Medical (ISM), and mobile communication, etc., while most of the higher portion of the spectrum is still not utilized, and can be exercised for 5G technology [13].

However, focusing on the higher portion of the spectrum has also raised some challenges for this 5G technology. One of the challenges is the free space propagation of these frequencies, as the signals at the lower frequency propagate for more than tens of miles and can easily penetrate through high tall buildings and trees. On the other hand, the signals at higher frequency bands can travel only a few miles and cannot penetrate through dense materials very well, resulting a lower coverage area. Nevertheless, these properties are not essentially being disadvantaged [14]. These propagation losses can be exploited to increase the frequency reuse, by introducing the small cell base stations known as pico-cells and femtocells. Another challenge in the wireless communication at the higher frequencies is the rain and the atmosphere which make these higher frequencies impractical [15,16]. In other words, these frequencies are badly affected by rain, snowfall and fog, etc. Thus, the electromagnetic (EM) waves experience higher losses in terms of signal quality and strength, etc., by these atmospheric attenuations [17]. However, this problem can be resolved by designing the antenna, which is highly directive and possesses a high gain [18,19].

In the literature [20–28], different MIMO antennas have been reported; covering the wide range of frequencies of the 5G targeted spectrum. Some of them have proposed the MIMO configuration for lower portion of spectrum i.e., below 6 GHz while above 20 GHz frequency, the MIMO configuration has also been presented. In [20], the four-antenna structure is implemented, covering the 5G mm-wave frequency band from 25.5–29.6 GHz with a peak gain of 8.3 dB. Similarly, a MIMO array with an effective bandwidth of 3.4 to 3.6 GHz at -6 dB reference is proposed in [21] for 5G applications. The total volume of the proposed antenna is $145 \times 75 \times 6$ mm^3. Moreover, the MIMO antenna system with a total volume of $90 \times 90 \times 1.6$ mm^3 is proposed in [22]. The proposed antenna possesses the impedance bandwidth of 3 to 9 GHz. In [23], a dual band MIMO antenna array having dimensions of $150 \times 75 \times 7$ mm^3 is presented, with a bandwidth of 3.4 to 3.6 GHz and 4.8 to 5.1 GHz at -6 dB reference. Likewise, a MIMO antenna array for millimeter wave communication with a SIW fed slotted is presented in [24]. The proposed antenna covers the 27.5–28.35 GHz and 24.25–27.5 GHz frequency bands for 5G, whereas the gain alters from 8.2 to 9.6 dB over the desired wideband region. In [25], a high gain MIMO antenna for 5G applications is presented, which covers the frequency band ranging from 26–29.5 GHz. The peak gain achieved is 14 dB. Similarly, in [26], a 5G metamaterial-based antenna for MIMO systems with a maximum gain value of 7.4 dB at the 26 GHz frequency band is presented. A broadband MIMO antenna with an impedance bandwidth of 2.6 to 13 GHz is reported in [27], while the overall size of the proposed antenna is $66.8 \times 40 \times 0.8$ mm^3. Likewise, in [28], the four element MIMO antenna system covering the 5G frequency band 27.5 to 40 GHz with an

overall size of 158×77.8 mm^2 is proposed. It is observed from the above literature review that the MIMO configuration presented is either large or complex in structure. Furthermore, the reported antennas [20–28] possess poor bandwidth due to which the number of frequency channels gets limited, while some of them also achieve low gain at the desired frequency band, which is an important factor at the mm-wave spectrum.

In this paper, a quad element MIMO antenna for 5G mm-wave applications is demonstrated. The proposed antenna possesses a wideband and high gain with a good MIMO characteristic for 5G millimeter wave applications. The wideband of the antenna is further helpful to achieve a high data rate transmission. The radiating elements of the proposed MIMO antenna design consist of four different arcs which mainly contribute in achieving a wideband performance. Moreover, the proposed MIMO configuration antenna elements are orthogonally assembled to each other, while the elements in diagonal position are assembled in the anti-parallel mode to lower the mutual interference between the MIMO antenna elements. Furthermore, to ensure that the proposed MIMO antenna system contains the same voltage; the antenna elements ground surfaces are connected. The remaining research work is sequenced in the following way. Section 2 presents the geometry of the proposed MIMO antenna and discussion is also made on the design evolution steps of the antenna element. Results are discussed in Section 3, while Section 4 concludes the paper.

2. Antenna Geometric Configuration and Design

The proposed quad element MIMO antenna is printed on RT-5880 substrate with a loss tangent and relative permittivity of 0.0009 and 2.2, respectively, whereas its thickness is 1.57 mm. The geometrical layout of the proposed MIMO configuration is illustrated in Figure 1, while Table 1 provides the dimensions of different design parameters. The proposed MIMO configuration consists of four antenna elements. A finite ground plane made up of copper with a size of 80 mm $\times$ 80 mm is used to back the substrate. Copper with a very stable conductivity of 5.8×10^7 S/m is used for the radiating element. Due to the very stable conductivity of copper, its effect on the impedance matching is very low. All the simulations and modeling of the proposed MIMO configuration are carried out in the CST Microwave Studio software.
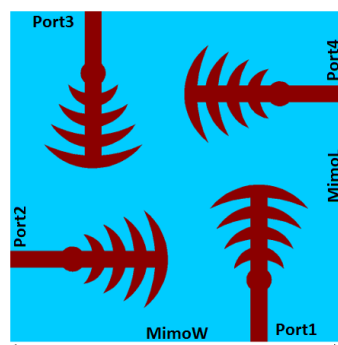
Figure 1. Proposed wideband multiple-input multiple-output (MIMO) antenna geometric layout.

Table 1. Proposed wideband antenna element dimensions.

Parameter	Value (mm)	Parameter	Value (mm)
SubW	40	Arc4	6.0
SubL	40	FeedL	12.76
FeedW	4.0	FW	2.15
Arc1	15	FL	2.54
Arc2	15	Rad	3.0
Arc3	9.0	MimoL	80
MimoW	80	–	–

2.1. Single Antenna Element Design

The schematic of the unit antenna element with a size of 40×40 mm², as illustrated in Figure 2, serves as a building block for the four port or quad element MIMO antenna. The substrate of the antenna element is backed by a full ground plane to reduce to the flow of the antenna radiated waves in the backward direction and to achieve a maximum gain.
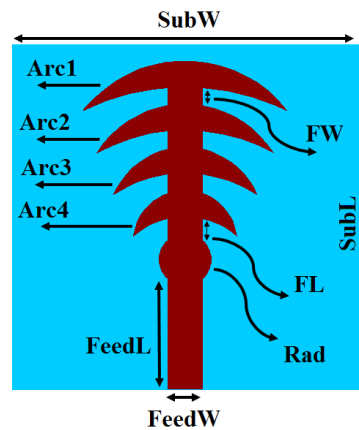

Figure 2. Layout of the proposed wideband antenna element.

The number of arcs and their dimensions must be carefully chosen to achieve the proper wideband response for the desired frequency range. The arc-shaped stripe is evolved from a circular patch as shown in Figure 3. First of all, a simple circular patch geometry is approximated by using the standard theory of circular patch antenna [29], i.e.,

$$rad_1 = \frac{F}{\{1 + \frac{2h}{\pi \epsilon_r F}[\ln(\frac{\pi F}{2h}) + 1.7726]\}^{1/2}} \tag{1}$$

$$F = \frac{8.791 \times 10^9}{f_r \sqrt{\epsilon_r}} \tag{2}$$

Then, the arc-shaped stripe is optimized and evolved for the targeted mm-wave spectrum by subtracting the circular patch step by step.
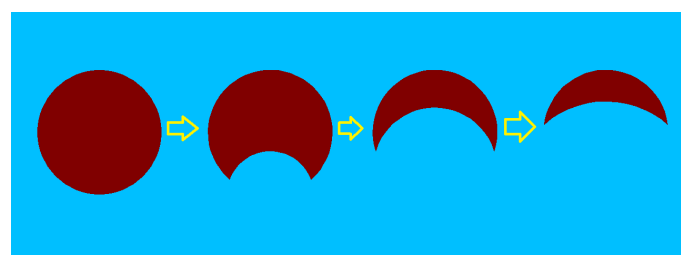

Figure 3. Arc-shaped stripe design evolution from a circular patch.

The evolution of the antenna element for the proposed MIMO system is discussed, as depicted in Figure 4. The design process consists of four antennas, i.e., Antenna-A, Antenna-B, Antenna-C and Antenna-D. Figure 4a illustrates the geometry of Antenna-A which is the basic monopole structure widely used in variant shapes as reported in [30–34], while Figure 4d depicts the geometry of Antenna-D; the proposed unit antenna which is used for the quad element MIMO antenna. The reflection coefficient (S_{11}) at -10 dB reference for these different design stages is depicted in Figure 5.

At the first stage, Antenna-A with just single arc-shaped stripe is designed on the top of the substrate as shown in Figure 4a, which shows an approximately wideband response above 31 GHz, whereas, below that frequency, a single resonance is obtained at the 28.5 GHz frequency band. Thus, at the second stage, Antenna-B with two arc-shaped stripes is produced to improve the response of the antenna element as illustrated in Figure 4b. This time a wideband response is observed for the frequency band of 23 to 34.8 GHz and 36.5 GHz to onwards. To improve the response further, Antenna-C with three arc-shaped stripes is introduced at stage three as depicted in Figure 4c, which gives a satisfactory wideband ranging from 23.2 to 39.2 GHz. Finally, at stage four, Antenna-D with four arc-shaped stripes is designed as shown in Figure 4d, to observe the effect on wideband response obtained at stage three. However, it is worth mentioning that the arc-shaped stripe introduced at stage four does not have a major effect on the wideband response achieved at stage three. Thus, a final geometry containing four different arc-shaped stripes is achieved, shown in Figure 4d for the MIMO configuration. Figure 6a–c illustrate the surface current distribution at the 28 GHz, 33 GHz and 38 GHz frequency bands, respectively. It is observed that the entire effective resonant length of the proposed antenna element is responsible for achieving the wideband characteristics.

(**a**) (**b**) (**c**) (**d**)
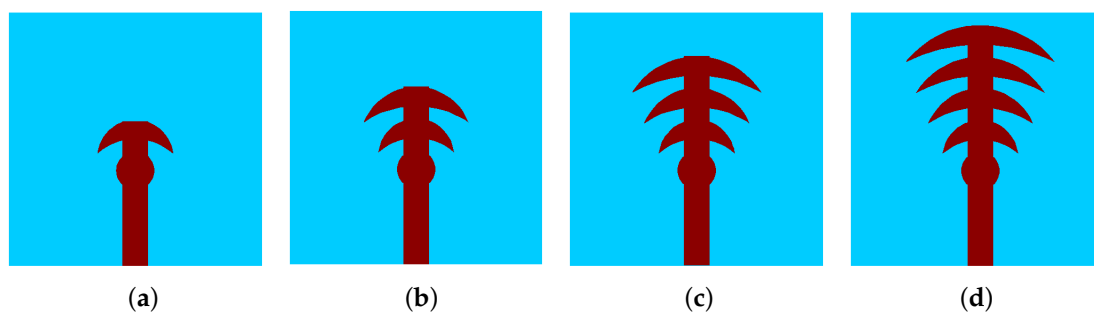
Figure 4. Geometrical design evolution steps of the proposed wideband antenna element. (**a**) step 1 Antenna-A). (**b**) step 2 (Antenna-B). (**c**) step 3 (Antenna-C). (**d**) step 4 (Antenna-D).
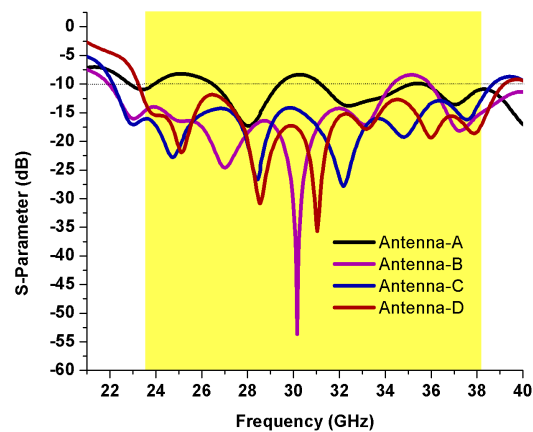
Figure 5. Reflection coefficient comparison of the different geometrical design evolution steps.

It is evident from the comparison of the simulated scattering-parameter (reflection coefficient) or (S_{11}) that the unit antenna exhibits improvement in the impedance bandwidth by adding additional arch-shaped stripes. It is evident that bending, meandering and tapering the monopole antenna design gives excellent properties such as compactness and less complex structure having multiple frequency bands at a reasonable cost of production [30–34]. However, the reported structure can be further improved to accommodate the higher frequency bands for 5G communication systems. Thus, inspired by the related work [30–34], a new tree-shaped quad element MIMO antenna is conceived.
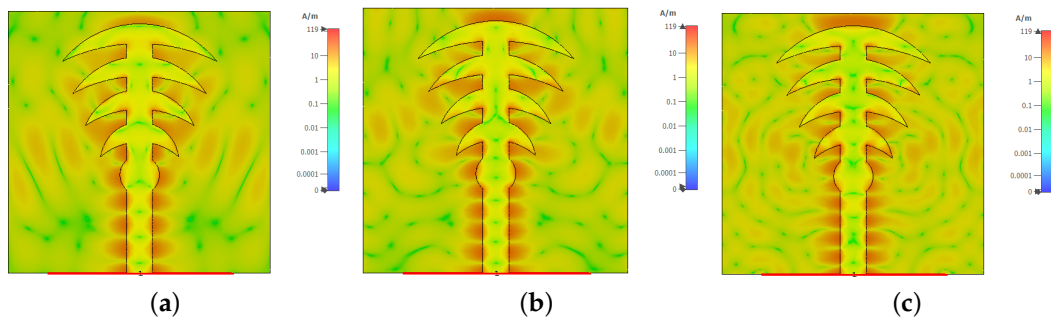
Figure 6. Wideband antenna element current distribution at (**a**) 28 GHz, (**b**) 33 GHz, and (**c**) 38 GHz.

2.2. Integeration of Four Unit Antenna for MIMO Configuration

In this section, a quad element MIMO antenna is built as depicted in Figure 1, by using the unit antenna element design obtained in the previous section. The individual antenna element occupies an area of 40×40 mm^2, are placed symmetrical and rotational in the 90-degree interval, forming a square shape. The ports isolation of greater than 20 dB is achieved for the proposed MIMO antenna. This is consistent with a fact that most of the current is concentrated in the parasitic arc shape stripes for each port excitation with less propagation to other ports as shown in Figure 7.
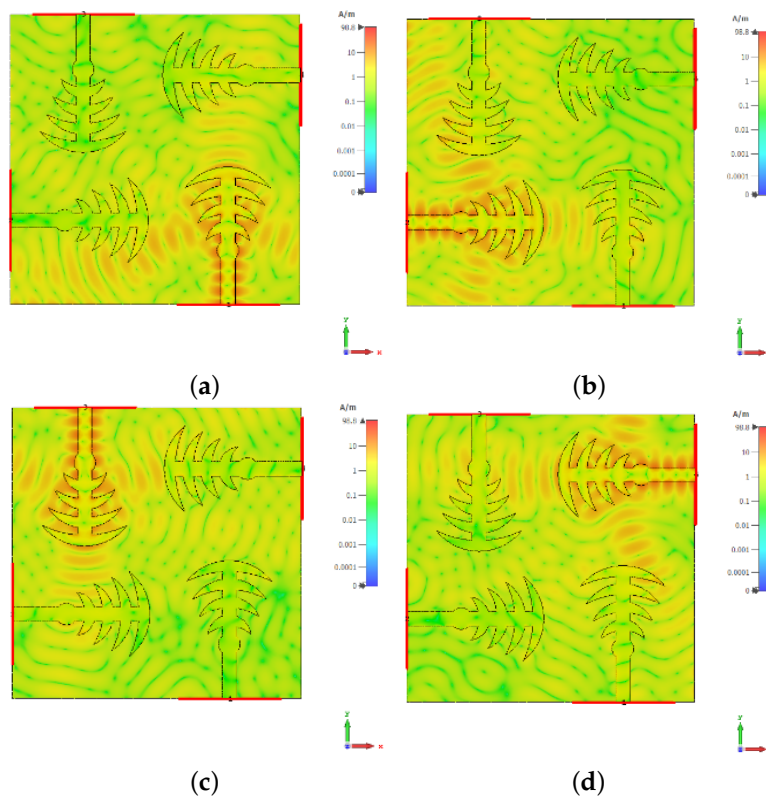

Figure 7. MIMO antenna system current distribution at 28 GHz for (**a**) port 1, (**b**) port 2, (**c**) port 3, and (**d**) port 4.

The mutual interference among the radiating elements makes the designing of the quad port diversity antenna complex task. The presence of manifold similar elements in the MIMO configuration leads to multiple increases in the mutual interference and Envelope Correlation Coefficient (ECC) among different antenna elements. That is why the placement of diagonal elements in the anti-parallel mode for the quad element MIMO antenna is chosen, while the four elements are assembled orthogonally to each other. To ensure that the proposed MIMO wideband antenna ground plane contains the same voltage; the four monopole resonating elements ground surfaces are allied.

The prototype of the fabricated MIMO wideband 5G antenna is revealed in Figure 8. The surface current distribution of the four-port MIMO antenna on the excitation of all ports sequentially at the frequency 28 GHz is depicted in Figure 7. It is observed that the current flow is mainly concentrated along the edges of arcs and around the feedline of the proposed MIMO antenna elements. Moreover, the concentration of the coupling current among the elements of MIMO antenna is insignificant.
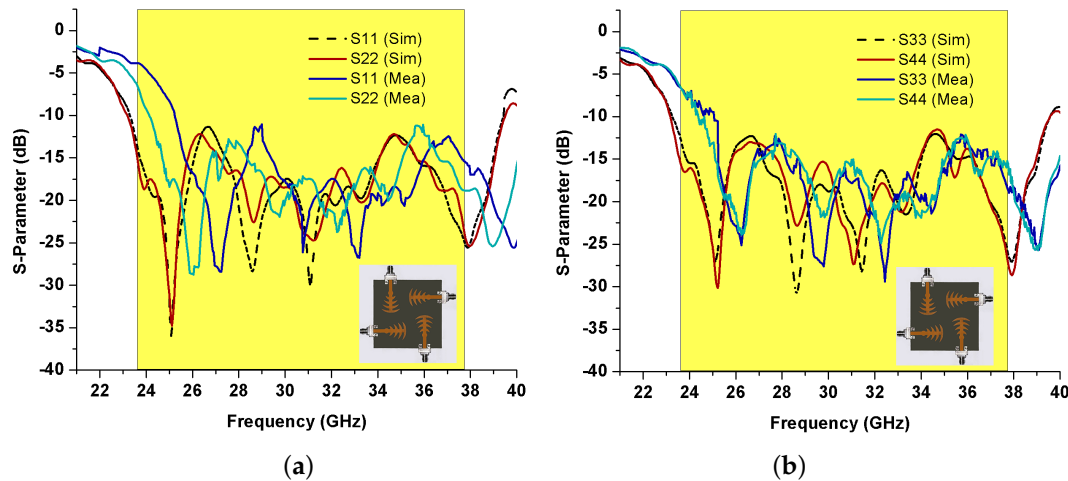

Figure 8. Proposed wideband MIMO antenna reflection coefficients: (**a**) port 1 and 2; (**b**) port 3 and 4.

3. Measured Results

The detailed analysis of the measured and simulated results is performed in this section. The southwest RF connector is used to feed the MIMO antenna elements. The antenna measurements are carried out using Agilent 8722ES vector network analyzer. While measuring transmission and reflection coefficient for the fabricated quad element MIMO antenna, the idle ports are terminated in 50 Ω load. The same procedure is adopted for the radiated far-field measurement in the anechoic chamber.

3.1. S-Parameters

A good coherence in the simulated and measured reflection coefficients is observed with a slight shift in the frequency bands due to the use of cables during the measurement or fabrication losses as shown in Figure 8. It is noted that the impedance bandwidth based on −10 dB criterion of the proposed MIMO antenna is 23 to 40 GHz. The mutual interference among the MIMO antenna elements is well above 20 dB for the entire desired wideband region, as depicted in Figure 9.
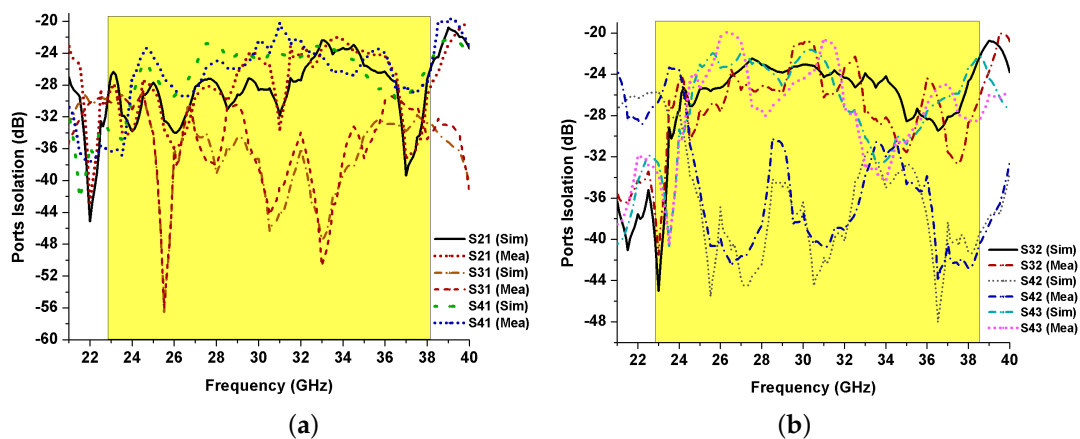

Figure 9. Proposed wideband MIMO antenna S-parameters at (**a**) port 1 and (**b**) other port.

3.2. Far Field Measurment

The measured radiation patterns for two principal planes, namely E-plane and H-plane at 28 GHz, 33 GHz and 38 GHz are shown in Figure 10. The radiating elements of the proposed MIMO antenna by virtue of its orthogonal placement have pattern diversity which is helpful to mitigate the multipath effect for communication systems. The MIMO antenna system exhibits directional radiation patterns. The proposed antenna overall possesses a good resemblance in the simulated and measured radiation patterns. Although the inconsistencies between the measured and simulated data are noted due to the cable losses and fabrication errors. The measured gain noted for Antenna-1 (port1) at 28, 33 and 38 GHz is 10.58, 8.87 and 11.45 dB, respectively while for the Antenna-2 (port2), Antenna-3 (port3) and Antenna-4 (port4); the measured gain of above 9 dB is obtained for the entire desired wideband region. However, the peak gain of the proposed MIMO antenna is observed at 12 dB, as illustrated in Figure 11. The measured and simulated totally efficiency of the MIMO antenna is presented in Figure 12. The measured total efficiency of greater than 70% is achieved for the overall desired wideband.
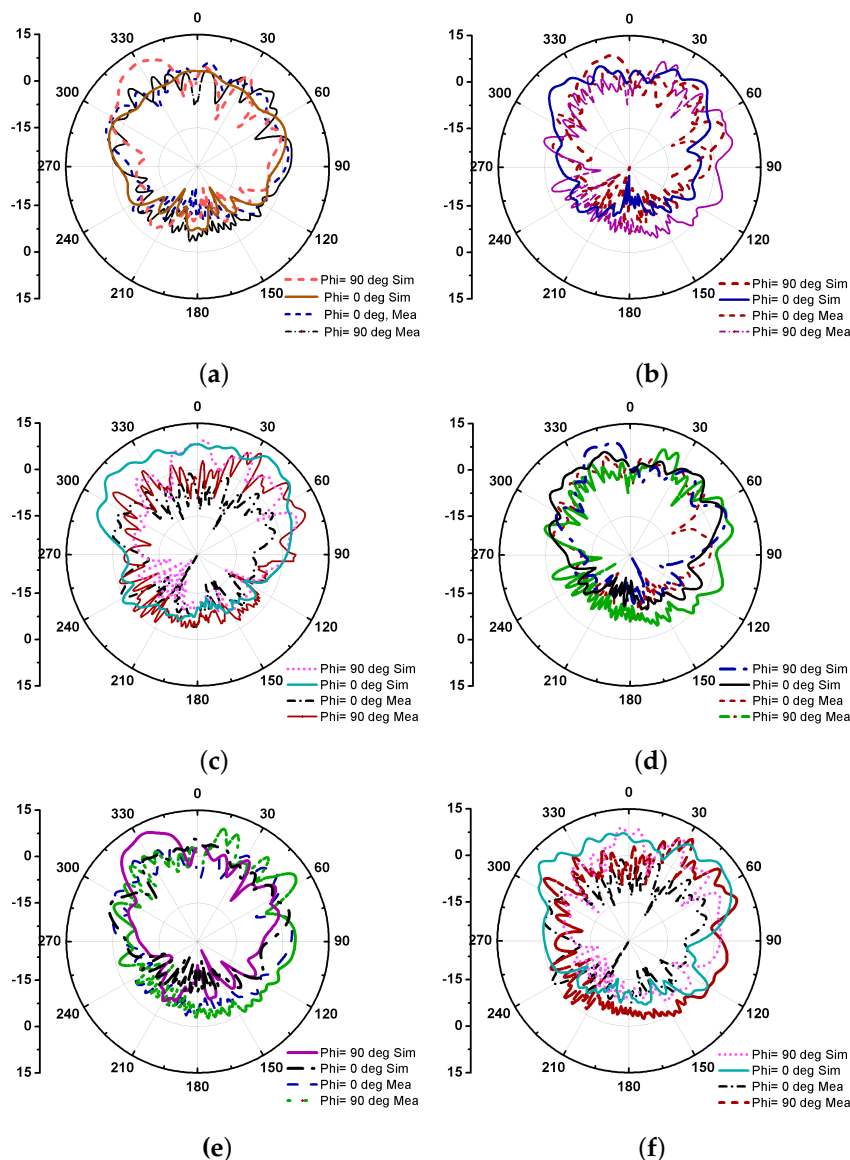
Figure 10. Radiation patterns of MIMO antenna: (**a**) port-1/28 GHz; (**b**) port-1/33 GHz; (**c**) port-1/38 GHz; (**d**) port-2/28 GHz; (**e**) port-2/33 GHz; (**f**) port-2/38 GHz.
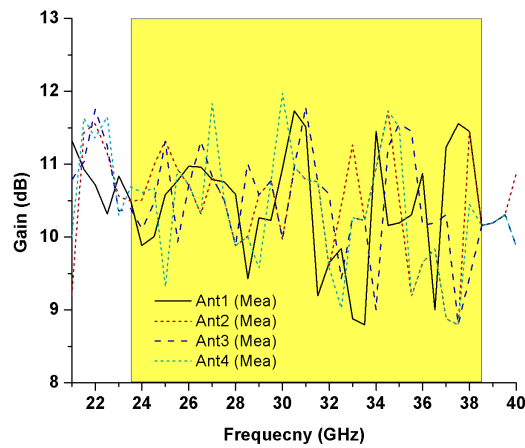
Figure 11. Maximum gain over frequency of the MIMO antenna elements.
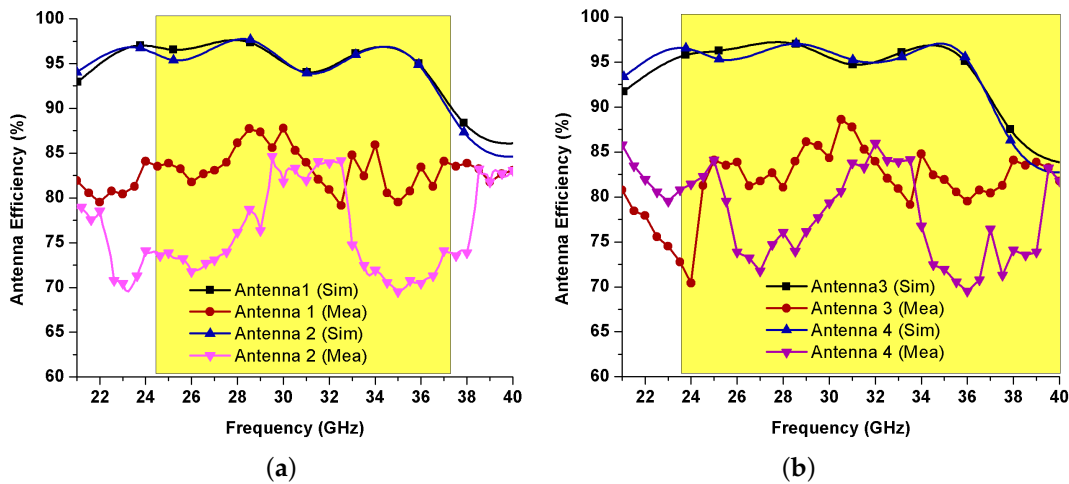
Figure 12. Efficiencies of the proposed MIMO antenna system: (**a**) antenna 1 and 2; (**b**) antenna 3 and 4.

3.3. MIMO Performance Metrics for the Quad Antenna System

The essential MIMO performance metrics such as the Mean Effective Gain (MEG) and Envelope Correlation Coefficient (ECC) for the proposed MIMO antenna system are discussed in this section. Figure 13 shows the ECC between the different ports of the MIMO antenna. The following expression [35] can be employed to compute the ECC between port 1 and port 2 of the quad element MIMO antenna:

$$\rho_{eij} = \frac{|S_{ii} \times S_{ij} + S_{ji} \times S_{jj}|^2}{(1 - |S_{ii}|^2 - S_{ij}^2)(1 - |S_{ji}|^2 - S_{jj}^2)} \tag{3}$$

Likewise, the ECC between the MIMO antenna other ports can be computed as well. It is observed that the ECC is below 0.0014 for the entire wideband region, obeying the practical standard of <0.5 required for the optimal diversity performance and ensuring independent channel operation.

Figure 13. Envelope Correlation Coefficients (ECCs) between some adjacent antenna-elements.

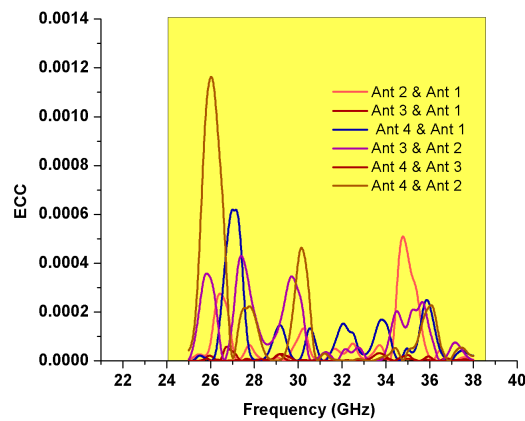The antenna elements mutual interaction and statistical properties of the propagation environment are quantified by MEG. The MEG is helpful to understand the power imbalance by considering the vital parameters such as total efficiency, gain and propagation environment in multiple branches or multiple antenna elements, degrading the diversity performance. To fulfil the balance power standard and for optimal diversity performance with a good channel characteristic; the difference between MEGs of any two antennas equal should be less than 3 dB. The numerically estimated values of MEG calculated using Equation (4), [20] are tabulated in Table 2. The terms *i* and *k* represent the antenna under observation and number of antennas, respectively. The MEG calculated based on measured results meet the required standard with the ratio of any two MEGs of the proposed quad element MIMO antenna being nearly equal to 1.

$$MEG_i = 0.5(1 - \sum_{j=1}^{k} S_{ij}) \tag{4}$$

Table 2. MEG for Antenna-1 to Antenna-4.

Frequency (GHz)	XPR	MEG Ant.1 (dB)	MEG Ant.2 (dB)	MEG Ant.3 (dB)	MEG Ant.4 (dB)
28	1	−5.24	−5.36	−5.45	−5.33
	6	−6.13	−6.34	−6.53	−6.64
33	1	−5.32	−5.43	−5.34	−5.37
	6	−6.63	−6.43	−6.33	−6.67
38	1	−5.88	−5.83	−5.65	−5.56
	6	−6.87	−6.31	−6.26	−6.34

The comparison of the proposed wideband MIMO antenna for 5G applications and other antennas reported in the literature is presented in Table 3. It is observed from the comparison that the proposed MIMO antenna owns numerous advantages over the previously reported MIMO antennas [20–28], in terms of total efficiency, impedance bandwidth, isolation among MIMO antenna elements, number of radiating elements, and gain. Furthermore, the radiating elements are assembled in the anti-parallel mode and orthogonally to provide better isolation among antenna elements, while the proposed quad element MIMO antenna possesses a common ground plane to achieve a stable operation.

Table 3. Performance comparison with previous published literatures.

Ref.	Ports	Bandwidth (GHz)	Peak Gain (dB)	Size (mm^3)	Isolation (dB)	Total Eff. (%)	ECC
[20]	4	25.5–29.6	8.3	$30 \times 35 \times 0.76$	>10	80–85	<0.01
[21]	8	3.4–3.6	1.6–4.5	$145 \times 75 \times 6$	>15	42–73	<0.16
[22]	4	3-9	11–12	$90 \times 90 \times 1.6$	>13	–	–
[23]	8	3.4–3.6, 4.8–5.1	–	$150 \times 75 \times 7$	>11.5	48–85	<0.08
[24]	–	21–34	9	–	–	–	–
[25]	4	26–29.5	14	$19 \times 19 \times 7.608$	>20	–	<0.015
[26]	–	24–28	7.4	$30 \times 30.5 \times 0.508$	–	–	–
[27]	2	2.6–13	0.76–6.02	$66.8 \times 40 \times 0.8$	>15	>75	<0.02
[28]	4	27.5–40	5.8–7.2	$158 \times 77.8 \times 0.381$	>17	<75	<0.001
Prop.	4	23–40	12	$80 \times 80 \times 1.57$	>20	>70	<0.0014

4. Conclusions

In this paper, a quad element MIMO antenna for 5G mm-wave applications is demonstrated. The proposed antenna possesses a wideband and high gain with a good MIMO characteristic for 5G mm-wave applications. The operation band of the proposed antenna covers from 23 GHz to 40 GHz. Each radiating element of the proposed MIMO configuration contains four different arc-shaped stripes which help to achieve the wide bandwidth and high element isolation of more than 20 dB. The peak gain of 12 dB is achieved for the proposed MIMO antenna. The high gain of the proposed antenna can be further helpful to overcome the atmospheric attenuations face by the higher frequencies. The mean effective gain and envelope correlation coefficient are also provided for the proposed MIMO configuration. In addition, the measured total efficiency of the proposed MIMO antenna is observed to be above 70% for the desired millimeter wave frequencies. Apart from this, the prototype of the MIMO wideband antenna is fabricated and tested. A good coherence between the experimental and simulated results is achieved. The proposed MIMO antenna operates efficiently with a significant return loss, wide bandwidth, high gain and high element isolation, which make it a potential candidate for 5G mm-wave applications.

Author Contributions: Conceptualization, D.A.S. and S.H.K.; methodology, D.A.S.; Software, D.A.S., S.H.K. and A.A.; Validation, M.A., F.M.; Formal Analysis, F.M., M.A.; Investigation, F.M., M.I., A.G., S.R.; Resources, A.A., M.T., M.I., S.R., and A.G.; Data Curation, D.A.S.; writing—original draft preparation, D.A.S.; writing—review and editing, D.A.S., M.A., S.H.K.; F.M., and M.T., Visualization, D.A.S; supervision, M.A.; project administration, M.A., M.I., and A.G. All authors have read and agreed to the published version of the manuscript.

Conflicts of Interest: The authors declare no conflict of interest.

References

1. Sharaf, M.H.; Zaki, A.I.; Hamad, R.K.; Omar, M.M.M. A novel dual-band (38/60 GHz) patch antenna for 5G mobile handsets. *Sensors* **2015**, *20*, 2541. [CrossRef]

2. Haroon, M. S.; Muhammad, F.; Abbas, G.; Abbas, Z.H.; Kamal, A.; Waqas, M.; Kim, S. Interference Management in Ultra-Dense 5G Networks with Excessive Drone Usage. *IEEE Access* **2020**, 1–10. [CrossRef]

3. Khan, J.; Sehrai, D.A.; Ali, U. Design of dual band 5G antenna array with SAR analysis for future mobile handsets. *J. Electr. Eng. Technol.* **2019**, *14*, 809–816. [CrossRef]

4. Pervez, M.M.; Abbas, Z.H.; Muhammad, F.; Jiao, L. Location-based coverage and capacity analysis of a two tier HetNet. *IET Commun.* **2017**, *11*, 1067–1073 [CrossRef]

5. Sun, L.; Li, Y.; Zhang, Z.; Feng, Z. Wideband 5G MIMO antenna with integrated orthogonal-mode dual-antenna pairs for metal-rimmed smartphones. *IEEE Trans. Antennas Propag.* **2020**, *68*, 2494–2503. [CrossRef]

6. Abdullah, M.; Kiani, S.H.; Iqbal, A. Eight element multiple-input multiple-output (MIMO) antenna for 5G mobile applications. *IEEE Access* **2019**, *7*, 134488–134495. [CrossRef]

7.   Yuan, X.; He, W.; Hong, K.; Han, C.; Chen, Z.; Yuan, T. Ultra-wideband MIMO antenna system with high element-isolation for 5G smartphone application. *IEEE Access* **2020**, *8*, 56281–56289. [CrossRef]

8.   Altaf, A.; Alsunaidi, M.A.; Arvas, E. A novel EBG structure to improve isolation in MIMO antenna. In Proceedings of the IEEE USNC-URSI Radio Science Meeting (Joint with AP-S Symposium), San Diego, CA, USA, 9–14 July 2017; pp. 105–106.

9.   Wang, F.; Duan, Z.; Wang, X.; Zhou, Q.; Gong, Y. High isolation millimeter-wave wideband MIMO antenna for 5G communication. *Int. J. Antennas Propag.* **2019**, *2019*, 4283010. [CrossRef]

10.   Abdullah, M.; Kiani, S.H.; Abdulrazak, L.F.; Iqbal, A.; Bashir, M.A.; Khan, S.; Kim, S. High-performance multiple-input multiple-output antenna system for 5G mobile terminals. *Electronics* **2019**, *8*, 1090. [CrossRef]

11.   Haroon, M.S.; Abbas, Z.H.; Abbas, G.; Muhammad, F. SIR analysis for non-uniform HetNets with Joint decoupled association and interference management. *Comput. Commun.* **2020**, *155*, 48–57.

12.   Haroon, M.S.; Abbas, Z.H.; Muhammad, F.; Abbas, G. Coverage Analysis of Cell Edge Users in Heterogeneous Wireless Networks using Stienen's Model and RFA scheme. *Int. J. Commun. Syst.* **2019**, *33*, e4147. [CrossRef]

13.   Khan, J.; Sehrai, D.A.; Khan, M.A.; Khan, H.A.; Ahmad, S.; Ali, A.; Arif, A.; Memon, A.A.; Khan, S. Design and performance comparison of rotated Y-shaped antenna using different metamaterial surfaces for 5G mobile devices. *Comput. Mater. Contin.* **2019**, *60*, 409–420. [CrossRef]

14.   Wang, P.; Li, Y.; Song, L.; Vucetic, B. Multi-gigabit millimeter waves wireless communications for 5G: From fixed access to cellular networks. *IEEE Commun. Mag.* **2015**, *53*, 168–178. [CrossRef]

15.   Sulyman, A.I.; Alwarafy, A.; MacCartney, G.R.; Rappaport, T.S.; Alsanie, A. Directional radio propagation path loss models for millimeter-wave wireless networks in the 28-, 60-, and 73-GHz bands. *IEEE Trans. Wirel. Commun.* **2016**, *15*, 6939–6947. [CrossRef]

16.   Shayea, I.; Rahman, T.A.; Azmi, M.H.; Islam, M.R. Real measurement study for rain rate and rain attenuation conducted over 26 GHz microwave 5G link system in malaysia. *IEEE Access* **2018**, *6*, 19044–19064. [CrossRef]

17.   Zhang, J.; Ge, X.; Li, Q.; Guizani, M.; Zhang, Y. 5G millimeter-wave antenna array: design and challenges. *IEEE Wirel. Commun.* **2017**, *24*, 106–112. [CrossRef]

18.   Roh, W.; Seol, J.Y.; Park, J.; Lee, B.; Lee, J.; Kim, Y.; Cho, J.; Cheun, K.; Aryanfar, F. Millimeter-wave beamforming as an enabling technology for 5G cellular communications: Theoretical feasibility and prototype results. *IEEE Commun. Mag.* **2014**, *52*, 106–113. [CrossRef]

19.   Khalily, M.; Tafazolli, R.; Xiao, P.; Kishk, A.A. Broadband mm-Wave microstrip array antenna with improved radiation characteristics for different 5G applications. *IEEE Trans. Antennas Propag.* **2018**, *66*, 4641–4647. [CrossRef]

20.   Khalid, M.; Iffat Naqvi, S.; Hussain, N.; Rahman, M.; Mirjavadi, S.S.; Khan, M. J.; Amin, Y. 4-port MIMO antenna with defected ground structure for 5G millimeter wave applications. *Electronics* **2020**, *9*, 71. [CrossRef]

21.   Liu, Y.; Ren, A.; Liu, H.; Wang, H.; Sim, C. Eight-port MIMO array using characteristic mode theory for 5G smartphone applications. *IEEE Access* **2019**, *7*, 45679–45692. [CrossRef]

22.   Haq, M.A.U.; Khan M.A.; Islam, M.R. MIMO antenna design for future 5G wireless communication systems. In *Software Engineering, Artificial Intelligence, Networking and Parallel/Distributed Computing*; Springer: Cham, Switzerland 2016; p. 653.

23.   Guo, J.; Cui, L.; Li, C.; Sun, B. Side-edge frame printed eight-port dual-band antenna array for 5G smartphone applications. *IEEE Trans. Antennas Propag.* **2018**, *66*, 7412–7417. [CrossRef]

24.   Yang, B.; Yu, Z.; Dong, Y.; Zhou, J.; Hong, W. Compact tapered slot antenna array for 5G millimeter-wave massive MIMO systems. *IEEE Trans. Antennas Propag.* **2017**, *65*, 6721–6727. [CrossRef]

25.   Hussain, N.; Jeong, M.; Park, J.; Kim, N. A broadband circularly polarized fabry-perot resonant antenna using a single-layered PRS for 5G MIMO applications. *IEEE Access* **2019**, *7*, 42897–42907. [CrossRef]

26.   Jiang, H.; Si, L.; Hu, W.; Lv, X. A symmetrical dual-beam bowtie antenna with gain enhancement using metamaterial for 5G MIMO applications. *IEEE Photonics J.* **2019**, *11*, 1–9. [CrossRef]

27.   Patre, S.R.; Singh, S.P. Broadband multiple-input–multiple-output antenna using castor leaf-shaped quasi-self-complementary elements. In *IET Microwaves, Antennas & Propagation*; IET: Hertford, UK, 2016; Volume 10, pp. 1673–1681.

28.   Abbas, E.A.; Ikram, M.; Mobashsher, A.T.; Abbosh, A. MIMO antenna system for multi-band millimeter-wave 5G and wideband 4G mobile communications. *IEEE Access* **2019**, *7*, 181916–181923. [CrossRef]

29. Balanis, C.A. *Antenna Theory: Analysis and Design*, 4th ed.; John Wiley and Sons: Hoboken, NJ, USA, 2016.

30. Deng, J.; Hou, S.; Zhao, L.; Guo, L. Wideband-to-narrowband tunable monopole antenna with integrated bandpass filters for UWB/WLAN applications. *IEEE Antennas Wirel. Propag. Lett.* **2017**, *16*, 2734–2737. [CrossRef]

31. Ding, K.; Gao, C.; Wu, Y.; Qu, D.; Zhang, B. A broadband circularly polarized printed monopole antenna with parasitic strips. *IEEE Antennas Wirel. Propag. Lett.* **2017**, *16*, 2509–2512. [CrossRef]

32. Alsariera, H.; Zakaria, Z.; Awang Md Isa, A. A broadband p-shaped circularly polarized monopole antenna with a single parasitic strip. *IEEE Antennas Wirel. Propag. Lett.* **2019**, *18*, 2194–2198. [CrossRef]

33. Wong, K.; Chang, H.; Chen, J.; Wang, K. Three wideband monopolar patch antennas in a Y-shape structure for 5G multi-input–multi-output access points. *IEEE Antennas Wirel. Propag. Lett.* **2020**, *19*, 393–397. [CrossRef]

34. Fang, X.; Wen, G.; Inserra, D.; Huang, Y.; Li, J. Compact wideband CPW-fed meandered-slot antenna with slotted Y-shaped central element for Wi-Fi, WiMAX, and 5G applications. *IEEE Trans. Antennas Propag.* **2018**, *66*, 7395–7399. [CrossRef]

35. Sharawi, M.S. Printed multi-band MIMO antenna systems and their performance metrics [wireless corner]. *IEEE Antennas Propag. Mag.* **2013**, *55*, 218–232. [CrossRef]